NANO LETTERS

2007
Vol. 7, No. 10
3138−3144

Persistence Length Measurements from Stochastic Single-Microtubule Trajectories

M. G. L. van den Heuvel, S. Bolhuis, and C. Dekker*

Kavli Institute of Nanoscience, Section Molecular Biophysics, Delft University of Technology, Lorentzweg 1, 2628 CJ Delft, The Netherlands

Received July 13, 2007; Revised Manuscript Received September 6, 2007

ABSTRACT

We present a simple method to determine the persistence length of short submicrometer microtubule ends from their stochastic trajectories on kinesin-coated surfaces. The tangent angle of a microtubule trajectory is similar to a random walk, which is solely determined by the stiffness of the leading tip and the velocity of the microtubule. We demonstrate that even a single-microtubule trajectory suffices to obtain a reliable value of the persistence length. We do this by calculating the variance in the tangent trajectory angle of an individual microtubule. By averaging over many individual microtubule trajectories, we find that the persistence length of microtubule tips is 0.24 ± 0.03 mm.

Introduction. Cytoskeletal molecular motors such as dynein, kinesin, or myosin use the energy of ATP hydrolysis to move unidirectionally along their associated protein filaments (microtubules for dynein and kinesin, actin filaments for myosin).[1] Cytoskeletal motors are involved in cellular organization, force generation, and directed intracellular transport of cargo,[2] and the use of these motor proteins for nanotechnological tasks is being explored.[3] The motility of motor proteins can be reconstituted in vitro in an inverted gliding assay.[4] Here, purified motor proteins are adsorbed onto a glass slide and subsequently bind to their cytoskeletal filaments, propelling them over the surface. By observing the motion of the filaments, various properties of the motor proteins, such as velocity, directionality, and processivity, have been studied.[5]

In this work, we use the inverted gliding assay to examine properties of the biofilaments themselves, in particular the stiffness of microtubule ends. Microtubules gliding over a kinesin-coated surface follow a random trajectory, the properties of which are determined by the fluctuations of the leading end. By measuring the mean-square deviation of the trajectory tangent angle as a function of time, we are able to infer the persistence length of the leading microtubule ends that have only submicrometer lengths.

It is of interest to measure the persistence length of short microtubule ends because microtubules show material properties on short length scales that deviate from the long length behavior.[6,7] Recently, it was measured that the persistence length of microtubules strongly decreased when the microtubule length was reduced.[7] This was inferred from observing thermal fluctuations of microtubule ends that were grafted on a substrate edge and had a fluorescent reporter bead attached to it. This method was used on microtubule lengths down to 3 μm. In gliding assays, the length of the leading microtubule end that extends beyond the last kinesin motor protein that binds to it can be even shorter depending on the surface concentration of motors. Observation of stochastic microtubule trajectories thus provides a convenient way of characterizing the persistence length of these short ends.

We present measurements of microtubule trajectories on unstructured kinesin-coated glass surfaces. We demonstrate that a measure of the persistence length can already be obtained from a single-microtubule trajectory. By averaging over multiple trajectories, we find that the persistence length of the taxol-stabilized microtubule ends is 0.24 ± 0.03 mm, which is indeed much shorter than expected for longer microtubules. This method provides a simple way to probe the magnitude of thermal fluctuations of microtubule ends that can be very short.

Stochastic Microtubule Trajectories. The trajectories of microtubules over a kinesin-coated surface obey statistics of a random walk.[8] As a microtubule is propelled, its leading end becomes progressively longer and is free to fluctuate through thermal agitation (Figure 1a). By doing so, the microtubule end explores a certain area ahead of it, where it will find a new kinesin to bind to. The range of fluctuations of the leading tip depends on the length and the stiffness of the microtubule end. The stiffness of the microtubule tip determines the curvature of the microtubule between adjacent

* Corresponding author. E-mail: dekker@mb.tn.tudelft.nl.

10.1021/nl071696y CCC: $37.00
Published on Web 09/21/2007

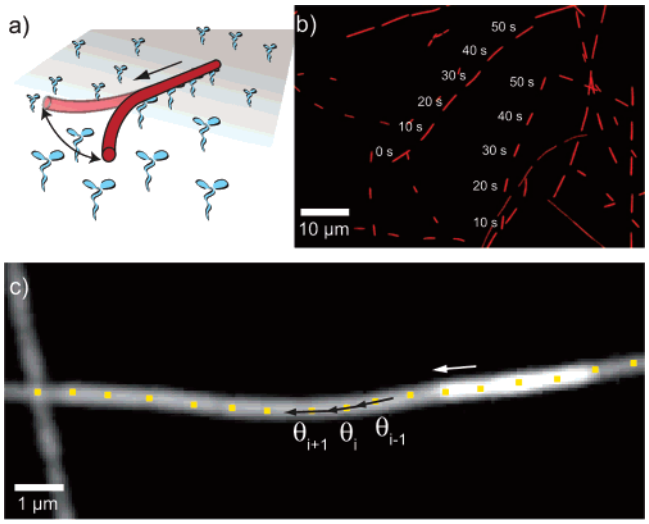

Figure 1. (a) Microtubules in a gliding assay follow a random trajectory due to thermal fluctuations of the leading tip. (b) Overlay of fluorescence images (with 10 s intervals) of microtubule gliding on a kinesin-coated glass substrate. (c) Zoom of a microtubule trajectory. The image was made by overlaying eight fluorescence images with 2 s intervals of a single microtubule with a length of 3 μm. One fluorescence image in the overlay has increased brightness to accentuate the microtubule. During the time of 14 s, the microtubule has traversed 10 μm. Superimposed are the coordinates of the leading tip of the microtubule, which are determined with 1 s intervals, using a fully automated MatLab routine. From the coordinates of the leading tip, tangent trajectory angles are determined at each step from the coordinates of the two adjacent time points.

motors and thus the curvature of the trajectory. We assume that the fluctuations of the microtubule tip are determined by the properties of the tip, while the remaining and largest part of the microtubule is fixated by the many bound kinesin motors distributed along its length (Figure 1a). The persistence length of the microtubule trajectory then equals the persistence length of the leading tip, provided the following two conditions are met:[8] (i) microtubules should be long enough to be attached to more than one kinesin at all times in order to prevent pivoting around a single motor, and (ii) the kinesin surface density should be high enough to prevent buckling of the microtubule tip when it is fluctuating.

Both conditions are met in our experiments. The first condition is fulfilled because we limit our experiments to microtubules that move without sudden changes of direction. In practice, this is the normal behavior for microtubules that are longer than 1 μm. This indicates that the distance between kinesin molecules bound to the microtubules is smaller than half this value. From this, we estimate that the surface density of active kinesin molecules is about 100 μm^{-2}.[9] This density is well above the critical limit at the which the microtubule end is expected to buckle, thus fulfilling the second condition.

We now relate the curvature of microtubule trajectories to the persistence length of the leading end. The orientations of a thermally fluctuating microtubule end of length d are Gaussian distributed around zero with a standard deviation $\sqrt{d/p}$, where p is the persistence length of the fluctuating end.[10] The trajectory of the microtubule is mapped out by the orientation of its leading end, and thus the variance of the trajectory tangent angle θ will increase on each consecutive displacement d_i. The evolution of θ can be described as a random walk, and after N steps, the variance in θ is given by $\mathrm{Var}(\theta) = \sum_{i=1}^{N}(d_i/p)$. After time t, the $\sum_{i=1}^{N} d_i = vt$, with v the speed of the microtubule, which yields a single expression for the time evolution of Var(θ):

$$\mathrm{Var}(\theta) = \frac{vt}{p} \qquad (1)$$

Note that the variance of the trajectory angle (eq 1) as a function of time is not dependent on kinesin density σ as long as the conditions apply that we previously mentioned ((i) microtubules should be attached to more than one kinesin at all times, and (ii) the kinesin surface density should be high enough to prevent buckling of the microtubule tip). The reason for this is that upon, say, increasing kinesin density, the variance of the trajectory angle per consecutive displacement decreases ($\propto (d_i/p) \sim (1/\sigma p)$[9]), but the number of steps that is required to traverse a certain distance increases in the same amount ($\propto (1/d_i) \sim \sigma$).

Single-Microtubule Trajectories. We use fluorescence microscopy to record time-lapse images of microtubules gliding over a kinesin-coated surface (Materials and Methods). We take fluorescence images with 1 s time resolution of an area that measures 87 $\times$ 66 μm^2. In Figure 1b, we show an overlay of fluorescence images with 10 s intervals that shows gliding motion of individual microtubules. The microtubules largely preserve their directionality during their trajectory, and only little curvature is present. From the image, it is thus clear that the persistence length of the microtubule ends is larger than the length of their trajectories ($\sim$30 μm in this image).

We use an automated tracing routine written in Matlab to determine the coordinates of the leading end of microtubules in consecutive frames. In this way, we obtain time-lapse trajectories of a large number of microtubules. In Figure 1c, we show an overlay of fluorescence images of an individual microtubule during 14 s, on which we superimposed the coordinates of its leading tip, as determined using our tracing routine. As expected, the coordinates of the leading tip overlap over the entire trajectory. From the coordinates of the leading microtubule tip, we calculate tangent angles θ at each time point of the trajectory from the coordinates of the two adjacent time points. In this way, we obtain a collection of angles, θ_1, θ_2, θ_3, ..., θ_N at times t_1, t_2, t_3, ..., t_N from an individual microtubule trajectory measured over $N + 2$ images.

We note that there is some uncertainty in the determination of the precise coordinates of the microtubule tip. This can be due to the optical blurring of the microtubule, its movement during the image recording ($\sim$70 nm during the 100 ms integration time of the camera), pixel discretization (65 nm), or the tracing routine. However, these errors are expected to be random and uncorrelated over time and will not have an effect on the measured variance of θ, except at zero time lag between the points for which the variance is calculated.[11]

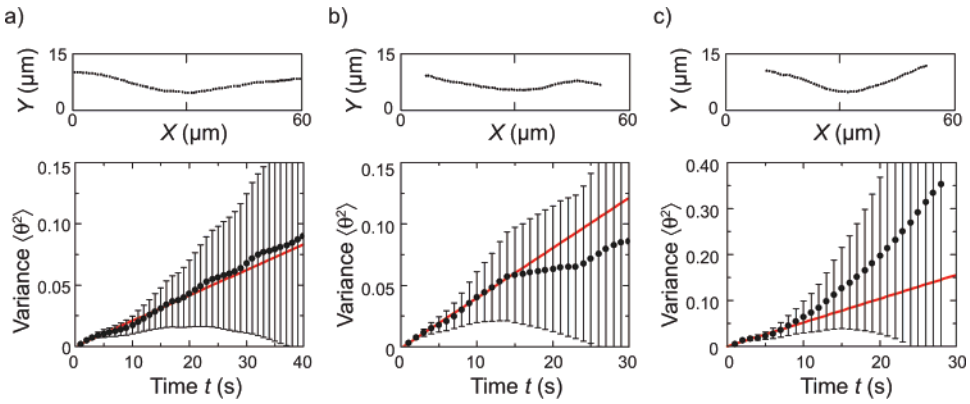

Figure 2. Single-microtubule trajectories were used to determine the variance of θ as a function of time by internal averaging. (a) Microtubule trajectory (upper panel) containing 97 datapoints. The calculated $\langle\theta^2(t)\rangle$ is shown in the lower panel. Red line is a weighed fits through points 1−9 s, which have expected relative errors less than 40%. (b) Similar data for a microtubule trajectory of 64 points, with a fit through points 1−6 s. (c) Microtubule trajectory containing 59 data points, with a fit through 1−6 s.

We now show that we can obtain an estimate of the variance of θ of even a single-microtubule trajectory. We do this using internal averaging of a microtubule trajectory, which is analogous to single-particle tracking experiments, in which the diffusional motion of a single particle is used to measure its diffusion coefficient.[11,12] We consider the calculation of the variance of θ as a function of time from a single trajectory of $N + 2$ images by averaging over all pairs of points in the trajectory with a certain time lag. Given the collection of tangent angles $\theta(n\Delta t)$, with Δt the time between the images and n any value from 1 to N, there are $N - n$ pairs that have a time lag $n\Delta t$, and the mean of the variance of θ at that time interval is:

$$\langle\theta^2(n\Delta t)\rangle = \frac{1}{N-n}\sum_{i=1}^{N-n}[\theta((n+i)\Delta t) - \theta(i\Delta t)]^2 \qquad (2)$$

Figure 2 shows three representative traces of microtubules trajectories, together with plots of $\langle\theta^2(t)\rangle$, obtained from these individual trajectories using eq 2. In Figure 2a, we show that $\langle\theta^2(t)\rangle$ increases linearly with time, as expected from eq 1. It should be noted that the error bars that are indicated on the data are much larger than the scatter in the data suggests. This is a result of two effects. First, the number of data points that is used to calculate $\langle\theta^2\rangle$ decreases with time and, second, the data points are not statistically independent.[11] As an illustration, the value of $\langle\theta^2(1)\rangle$ in Figure 2a is obtained from the average of $N - 1 = 96$ statistically independent pairs (eq 2). On the contrary, the value $\langle\theta^2(40)\rangle$ is obtained from only $N - 40 = 57$ individual measurements (i.e., $[\theta(41) - \theta(1)]$, $[\theta(42) - \theta(2)]$, ..., $[\theta(97) - \theta(57)]$, and these are highly correlated because they partially overlap, which results in the smooth variation of the variance as a function of time.

To estimate the error in $\langle\theta^2\rangle$ at each particular time, one needs to take into account this statistical correlation. An analysis in ref 11 estimated this error for a random walk in two dimensions, which can easily be extended to a one-dimensional random walk, as in our case for the trajectory angle θ. Consider that the value of θ is Gaussian distributed and that its mean-square deviation σ_θ^2 increases with time as vt/p (eq 1). Then, the variance to be expected in the mean-square deviation of θ^2 ($\mathrm{var}(\theta^2) = \langle(\theta^2 - \sigma_\theta^2)^2\rangle$) equals $2(vt/p)^2$,[11] and if θ^2 is calculated by averaging over different segments that are not statistically independent, then the expected variance in θ^2 was shown to be $2(vt/p)^2 \cdot 2n/3(N - n)$. Thus, if we take the standard deviation of θ^2 as the expected error, the relative error on each particular value of $\langle\theta^2(n\Delta t)\rangle$ follows as $\sqrt{4n/3(N-n)}$. This value for the expected relative error is valid as long as $n < N/2$.[11] The errors shown in Figure 2 where calculated using this formula.

The length of the microtubule trajectories varies significantly in our data. Obviously, it cannot exceed the size of the microscope field-of-view. In practice, it is limited by our automated tracing routine that cannot reliably track a microtubule if it crosses another microtubule. This frequently happens at the moderate microtubule densities, which we need to collect a statistically significant amount of data. Spontaneous detachment of microtubules from the surface was not a reason for limited trajectory lengths because this never happens at the high kinesin densities that we use. Another reason for ending a microtubule trajectory is that a microtubule gets pinned at the surface, presumably by a defect or an inactive kinesin motor, but this occurred only very infrequently. The resulting length distribution of trajectories is reminiscent of an exponential distribution, with approximately 70% of the trajectories having a length smaller than the mean trajectory length of 13 μm.

We obtain a value of the persistence length from individual microtubule trajectories from the slope of a weighted linear least-squares fit of eq 1 to the data, where the least-square residues are weighted inversely proportional to the error bars squared. We (arbitrarily) chose to include only those data points of each trajectory for which the estimated relative error in $\langle\theta^2(t)\rangle$ was less than 40%. Given the short lengths of our trajectories, the relative error increases fast for increasing time lag $n\Delta t$ and, at the chosen error margin, typically only 5−10 points, were included in each single-trajectory fit. Thus, this error margin is also an indication of the accuracy of the persistence length that we expect to derive from the

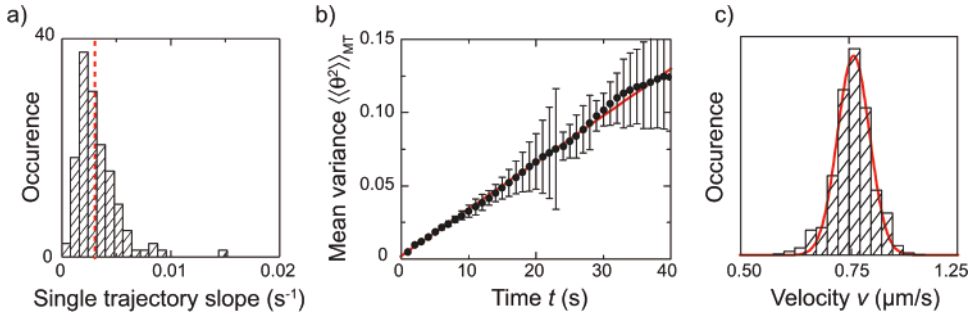

Figure 3. (a) Distribution of slopes obtained from 121 single-microtubule trajectories. The red line indicates the value of the slope that is obtained from panel (b). (b) Mean variance of θ as a function of time, calculated from the average of single-microtubule $\theta^2(t)$'s using eq 3. The error on the values of $\langle\langle\theta^2(t)\rangle\rangle_{MT}$. The red line is a weighed least-squares fit through data points 1−40 s. (c) Velocity of microtubules is normally distributed with 0.77 ± 0.09 μm/s (mean ± standard deviation).

individual slopes. From the fit to the data in Figure 2a (red line), we find a slope (2.1 ± 0.2) × 10^{-3} s^{-1}. The velocity of this microtubule was 0.75 ± 0.01 μm/s (mean ± standard error of the mean (SEM)), which results in a persistence length $p = 0.36 \pm 0.03$ mm for this particular microtubule. Similarly, we obtain from the trajectories in Figure 2b,c persistence length values of $p = 0.18 \pm 0.01$ mm, and $p = 0.15 \pm 0.02$ mm, respectively. Note that these errors represent only the least-squares errors of the linear fit, but that the actual error in p can be as large as 40%, given our choice to fit data points up to the time t where the expected standard deviation in $\langle\theta^2(t)\rangle$ reaches 40%.

Averaging over Multiple Trajectories. Although we demonstrate that individual microtubule trajectories allow one to determine the persistence length of the microtubule end, the statistical uncertainty in these values is relatively large because the length of the microtubule trajectories is experimentally limited. As we show in Figure 2, the expected relative error on $\langle\theta^2(t)\rangle$ can easily become larger than 40% for values of $\langle\theta^2(t)\rangle$ that are calculated for points along the trajectory that are separated by several seconds. For larger time lags $n\Delta t$, the number of segments that are used in the calculation of $\langle\theta^2(t)\rangle$ is limited and the expected relative error, $\sqrt{4n/3(N-n)}$, is large.

The statistical uncertainty in the determination of the persistence length from single-microtubule trajectories is apparent from the distribution of slopes that we determined from a large number of single-microtubule trajectories in a similar way as illustrated in Figure 2. The slopes were obtained by linear fits through those points of single-microtubule trajectories $\langle\theta^2(t)\rangle$ that have a relative error of less than 40%. In Figure 3a, we show the resulting distribution of slopes that was obtained from 121 trajectories. In accordance with the allowed error margin for the points included in the fitting procedure, the slopes are broadly distributed, with (3.2 ± 2.0) × 10^{-3} s^{-1} (mean ± standard deviation (STD)). We note that the standard deviation is larger (63% of the mean) than expected from the allowed relative error of 40% in the fits of the individual trajectories. This additional variance can be due to variations in the persistence length for different microtubules.

A more accurate estimate for the persistence length can be obtained by averaging the values of $\theta^2(t)$ from multiple microtubule trajectories. We construct a multitrajectory $\langle\langle\theta^2(t)\rangle\rangle_{MT}$ from an average over $\theta^2(t)$'s:

$$\langle\langle\theta^2(t)\rangle\rangle_{MT} = \left(\frac{1}{\sum_{1}^{M} N_j - n}\right) \sum_{j=1}^{M} \sum_{i=1}^{N_j - n} [\theta((n+i)\Delta t) - \theta(i\Delta t)]^2 \quad (3)$$

where the sum $\sum_{j=1}^{M}$ runs over all M microtubule trajectories j that each contain N_j data points. With respect to the expected error on the values of $\langle\langle\theta^2(t)\rangle\rangle_{MT}$, we note that a simple standard error of the mean will yield an underestimate for the reason that we previously discussed; a large number of θ^2's that enter in the sum of eq 3 are not statistically independent. On the other hand, an upper bound of the expected error can be found from considering the mean of the variances of the individual microtubule trajectories at each time point. Thus, as an upper bound, we approximate the error on each value of the multitrajectory average $\langle\langle\theta^2(t)\rangle\rangle_{MT}$ with the standard error of the mean of the absolute errors of the single trajectory $\langle\theta^2(t)\rangle$.

In Figure 3b, we show the average $\langle\langle\theta^2(t)\rangle\rangle_{MT}$ as obtained from averaging data from 885 individual microtubule trajectories. The magnitude of the errors is not monotonic as a function of time because not all trajectories that are used in the approximation of the errors have the same length. The red line is a weighted fit of eq 1 through the data, which yields a slope of (3.19 ± 0.04) × 10^{-3} s^{-1}. In agreement with the larger data set, this slope can be more accurately determined than from individual trajectories. As we indicate in Figure 3a, this value of the slope is slightly higher than the value corresponding with the peak of the distribution of single-trajectory slopes. We attribute this discrepancy to the limited and finite length of the individual microtubule trajectories, as we will discuss below.

To obtain the persistence length of the microtubule population, we determine the velocity of microtubules from their displacement between frames. As expected, the velocity of the microtubules is Gaussian distributed (Figure 3c) and has an average of 0.77 ± 0.09 μm/s (mean ± standard deviation). Using this value, we find an average persistence length $p = 0.24 \pm 0.03$ mm for the entire population.

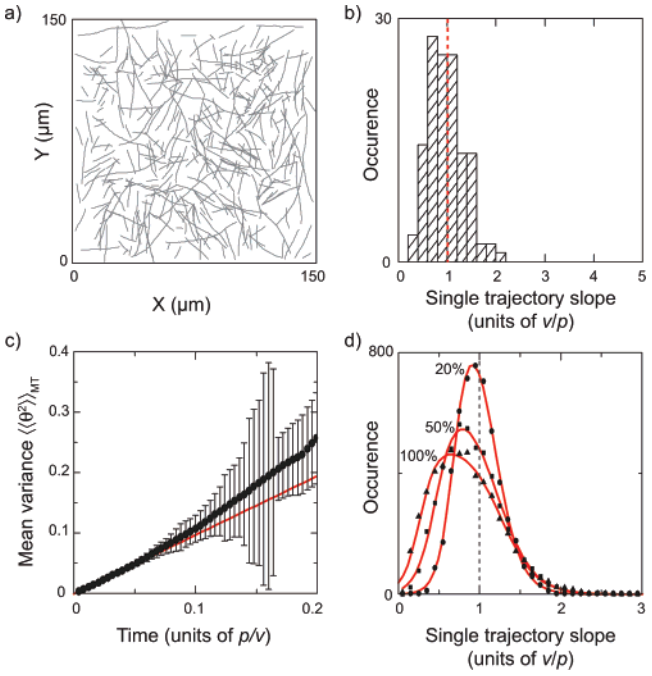

Figure 4. Simulation of stochastic microtubule trajectories (a) Selection of simulated microtubule trajectories with similar properties as the experimental data. (b) Distribution of slopes from simulated single trajectories. (c) Mean variance of θ as a function of time, calculated from the average of simulated single-microtubule trajectories. (d) Distributions of slopes from 5000 simulated single trajectories. The distributions of slopes were determined from the same data set, but the relative errors on the data points that were allowed in the single-trajectory fit were varied for each distribution, as indicated (dots, 20%; squares, 50%; triangles, 100%.)

Simulations of Stochastic Trajectories. We have determined a value of the persistence length of microtubule tips from individual microtubule trajectories as well as from an average over multiple microtubule trajectories. Additionally, we confirm the validity of this method by simulating the trajectories of a number of microtubule of known stiffness and subjecting it to the same analysis. In particular, we are interested in seeing if we can extract the value of the persistence length that we have entered in the simulations and whether we can assess the accuracy of the distribution of individual slopes. Previously, stochastic simulations of microtubule trajectories have been used to model their traversal through nanofabricated structures.[13]

We simulate a number of stochastic microtubule trajectories by calculating the stepwise progression of microtubules with Gaussian-distributed tip orientations that were taken from a distribution with standard deviation $\sqrt{d/p}$.[10] We use values for the microtubule velocity, time resolution, persistence length, the number of microtubule trajectories, and for length distribution of trajectories that are close to the experimental data.[14] The simulated microtubule trajectories were subsequently analyzed by using the same procedures as for the experimental data. As expected, we did not find any dependence on the kinesin density.

In Figure 4a, we show a selection of simulated microtubule traces. As expected, the trajectories are relatively straight because they are short compared to the persistence length of the microtubule tips. In our experiments, the trajectory lengths of microtubules are limited mainly by microtubule crossings, and for this reason we took a similar distribution of trajectory lengths for our simulations, of which Figure 4a gives a representative impression. Most microtubule trajectories are relatively short, with lengths of approximately 5−15 μm. We determine a distribution of slopes from individual microtubule trajectories as before, taking only those points with relative errors less than 40%. The distribution of slopes from 116 trajectories (Figure 4b), normalized to the expected value of v/p, is qualitatively similar to what we experimentally found, with a rather broad distribution of 0.98 ± 0.36 (mean ± standard deviation (STD) in units of the expected value of v/p). In Figure 4c, we show the multitrajectory average, which is obtained from the simulated data using eq 3. The features of the experimental data in Figure 3b are qualitatively reproduced, most notably the nonmonotonic increase of the error bars, and a deviation from linear behavior for larger times. A weighted linear fit yield 0.98 ± 0.01 in units of v/p.

The values that we find from the distribution of single-trajectory slopes and from the slope of the multitrajectory average are in good agreement with the value that we have entered into the simulation, which confirms the validity of our analysis. Moreover, we note that the standard deviation of the distribution of slopes 36% of the mean, which is close to 40% that is expected from the maximum relative error in the data that we allow in the fit from individual single-microtubule trajectories. From this, we confirm that the larger standard deviation in the experimental distribution of slopes (Figure 3a) most likely reflects an additional variance due to differences between individual microtubules. The value that we have determined from the experimental multitrajectory average (Figure 3b) is expected to form an accurate population average.

Finally, we want to confirm that the asymmetric distribution of experimental single-trajectory slopes is indeed due to the finite length of the trajectories as we previously surmised. Single-particle tracking applied to simulated two-dimensional Brownian motion has yielded similar results, with the distribution of slopes becoming increasingly wider and peaked toward lower values than expected upon increasing the number of points that were included in the fit.[12] To test this for the one-dimensional variable θ in our experiments, we simulate a large number of trajectories (5000) and we determine the distribution of single-trajectory slopes upon varying the maximum relative error that we allow in the data that is used for the fits of the slopes. Figure 4d shows the resulting distribution of slopes determined from single trajectories where the fit included data points that had an expected relative error of less than 20%, 50%, and 100%, respectively. It is clear that, upon allowing a larger error, the distribution of slopes becomes increasingly wider and peaked toward lower values, in agreement with the Brownian motion results in ref 12.

Discussion. We have shown that we can measure a value of the persistence length of the tips of single microtubules by tracing the coordinates of their leading tip. Calculation

of the variance of the tangent trajectory angles, together with internal averaging of the angles, provides a simple method to construct a $\langle\theta^2\rangle$ versus time plot for a single-microtubule trajectory. The correlation that is induced by internal averaging is estimated by attributing relative errors to the $\langle\theta^2\rangle$ data of magnitude $\sqrt{4n/3(N-n)}$.[11] By fitting the linear part of the $\langle\theta^2(t)\rangle$ data and by measuring the velocity of the microtubule, the persistence length of its tip can be calculated.

This method yields satisfactory results as long as the attributed relative errors are small, for which a relatively long trajectory is needed. For example, if a trajectory consists of $N = 100$ points, and a relative error of 40% in the value of $\langle\theta^2(t)\rangle$ is accepted, only the first $n = 10$ points can be used. If the acceptable error is 20%, only the first two or three points can be used. This inaccuracy is reflected in the width of the distribution of slopes that we determined from a large number of experimental single-microtubule trajectories. However, we find a distribution that is wider than expected, which could indicate variations between individual microtubules. We showed that, by averaging over multiple independent microtubule trajectories, we could obtain more accurate results. The consistency of our method was checked with simulations.

The persistence length $p = 0.24 \pm 0.03$ mm that we find for the microtubule ends in our experiments is much smaller than the value of 4−8 mm that is measured for long (5−50 μm) microtubules[15,16] but in agreement with the reducing trend that was observed by Pampaloni et al. down to microtubule ends of 3 μm.[7] This effect was attributed to shear deformation of microtubules due to sliding of adjacent protofilaments, which gives an extra compliance and that becomes dominant if the bending occurs on short length scales. In our experiments, we have varied the kinesin density over a factor of 10 (Materials and Methods), and we did not find a significantly different value of the persistence length in this range. Interestingly, two previous reports mention a value of the persistence length of microtubule trajectories but did not make a connection to the persistence length of the microtubule tip. Values of 0.1 mm[17] and 0.5 mm[18] were reported that agree well with the value that we find.

We recently obtained an independent measurement of the persistence length of microtubule ends by a different method, viz., by measuring the trajectory curvature of microtubules that were subjected to perpendicular electric forces. We related the curvature to the magnitude of the electric force and the average length of the microtubule tip, and we found that in these experiments $p = 0.55 \pm 0.22$ mm, which agrees reasonably with the value that we report here. However, our previous measurement relied on the measurement of the average tip length, which is hard to do very precisely, and on a calibration of the magnitude of the electric force. The method that we present here does not rely on other parameters.

Conclusions. We have demonstrated that we can obtain a measurement of the persistence length of microtubule ends by tracking of stochastic microtubule trajectories in gliding assays. The tangent angle of a microtubule trajectory can be described as a random walk, and the variance of the tangent angle increases linearly with time. We show that even a single-microtubule trajectory can yield a measurement of the persistence length if it is long enough and when internal averaging of the trajectory is used. By averaging the data over a large number of microtubule trajectories, we find a persistence length of the microtubule tip that is $p = 0.24 \pm 0.03$ mm. The value that we find for our microtubule ends, which we estimate to be of submicrometer length, is in good agreement with other recent data that reports a reduction of the persistence length for short microtubules.

Materials and Methods. Motility assays were performed as follows. A flow cell was assembled from two glass cover slips and double-sided tape and first incubated for 5 min with a casein solution (0.5 mg/mL casein in BRB80 buffer (80 mM Pipes, 1 mM $MgCl_2$, 1 mM EGTA, pH = 6.9). Second, a kinesin solution was perfused into the flow cell and incubated for 5 min. The concentration of our kinesin stock is 200 μg/mL, and the kinesin concentration in the solution that was added to the flow cell varied between 10 and 100 μg/mL. The kinesin was diluted in BRB80, supported with 0.2 mg/mL casein and 1 mM ATP. The data presented in the text were taken in a flow cell that was incubated with 40 μg/mL kinesin. Finally, the flow cell contents were exchanged with motility solution containing rhodamine-labeled paclitaxel-stabilized microtubules (~8 nM tubulin, 1 mM ATP, 1 mM $MgCl_2$, 10 μM Taxol, and antibleaching cocktail (20 mM D-Glucose, 0.020 mg/mL glucose oxidase, 0.008 mg/mL catalase, 1% β-mercaptoethanol)), all in BRB80 buffer. Microtubules were polymerized from 5 μL of bovine brain tubulin (4 mg/mL, 1 rhodamine labeled unit, 3 unlabeled units, Cytoskeleton, Denver, CO) in the presence of 4 mM $MgCl_2$, 1 mM GTP, and 5% DMSO in BRB80 buffer (37 °C for 45 min). Then the microtubules were stabilized and 400× diluted in BRB80 containing 10 μM Taxol.

References

(1) Schliwa, M.; Woehlke, G. *Nature* **2003**, *422*, 759.
(2) Vale, R. D. *Cell* **2003**, *112*, 467.
(3) van den Heuvel, M. G. L.; Dekker, C. *Science* **2007**, *317*, 333.
(4) Kron, S. J.; Spudich, J. A. *Proc. Natl. Acad. Sci. U.S.A.* **1986**, *83*, 6272.
(5) Howard, J.; Hudspeth, A. J.; Vale, R. D. *Nature* **1989**, *342*, 154.
(6) Kis, A.; Kasas, S.; Babic, B.; Kulik, A. J.; Benoit, W.; Briggs, G. A. D.; Schonenberger, C.; Catsicas, S.; Forro, L. *Phys. Rev. Lett.* **2002**, *89*, 248101.
(7) Pampaloni, F.; Lattanzi, G.; Jonas, A.; Surrey, T.; Frey, E.; Florin, E. L. Proc. *Natl. Acad. Sci. U.S.A.* **2006**, *103*, 10248.
(8) Duke, T.; Holy, T. E.; Leibler, S. *Phys. Rev. Lett.* **1995**, *74*, 330.
(9) Duke et al.[8] provide a relation between the average distance $\langle d\rangle$ of kinesin molecules bound to a microtubule and the surface concentration σ of active kinesins. It is assumed that kinesin motors can reach isotropically over a distance $w \approx 20$ nm to attach to a microtubule. If the motor density is very high, such that the microtubule tip can bend much less than its diameter, $\sigma \sim (1/\langle d\rangle w)$. If the surface density is lower, the microtubule end can explore a larger area and $\sigma \sim (\sqrt{p/\langle d\rangle^5})$, where p is the persistence length of the tip. The boundary between the two regimes is at $\sigma \sim w^{-5/3}p^{-5/3}$. If we estimate $\langle d\rangle \leq 0.5$ μm and $p \sim 0.5$ mm, then we find in both regimes that $\sigma \sim 10^2$ μm^{-2}, which is also approximately the value of σ^*, justifying the use of these relations. Finally, the critical kinesin surface density, below which buckling of the microtubule tip is expected to occur, is about 4 orders of magnitude lower than σ^*.
(10) Benetatos, P.; Frey, E. *Phys. Rev. E* **2003**, *67*, 051108.

(11) Qian, H.; Sheetz, M. P.; Elson, E. L. *Biophys. J.* **1991**, *60*, 910.
(12) Saxton, M. J. *Biophys. J.* **1997**, *72*, 1744.
(13) Nitta, T.; Tanahashi, A.; Hirano, M.; Hess, H. *Lab Chip* **2006**, *6*, 881.
(14) We simulated 1137 microtubule trajectories with a velocity that is Gaussian distributed with 0.78 ± 0.07 μm (mean ± STD). The distribution of simulated trajectory lengths was made similar to the experimental data by randomly picking a predetermind length for each simulated trajectory from an exponential distribution that resembled the experimental data. For the microtubule tip length, we assumed that it was exponentially distributed with mean 0.26 μm, although the length distribution of the tip is of no relevance to the evolution of the trajectory angle (eq 1). For the persistence length we took $p = 195$ μm. The coordinates of the microtubule after each step of random length were calculated based on its initial position, it momentarily tip length and tip orientation that were randomly picked from an exponential and Gaussian distribution, respectively. Afterwards, the positions of the leading tip were collected with 1 s intervals. We confirmed that adding a random variance onto the tip coordinates, representing the effects of pixel noise and errors in the tracing routine, did not affect the results.
(15) Gittes, F.; Mickey, B.; Nettleton, J.; Howard, J. *J. Cell Biol.* **1993**, *120*, 923.
(16) Janson, M. E.; Dogterom, M. *Biophys. J.* **2004**, *87*, 2723.
(17) Nitta, T.; Hess, H. *Nano Lett.* **2005**, *5*, 1337.
(18) Clemmens, J.; Hess, H.; Howard, J.; Vogel, V. *Langmuir* **2003**, *19*, 1738.

NL071696Y